Reduced Neuroinflammation Via Astrocytes and Neutrophils Promotes Regeneration After Spinal Cord Injury in Neonatal Mice

北出, 一季

Reduced neuroinflammation via astrocytes and neutrophils promotes regeneration after spinal cord injury in neonatal mice

Kazuki Kitade[1], Kazu Kobayakawa[1*], Hirokazu Saiwai[1], Yoshihiro Matsumoto[1], Kenichi Kawaguchi[1], Keiichiro Iida[1], Ken Kijima[1], Hirotaka Iura[1], Tetsuya Tamaru[1], Yohei Haruta[1], Gentaro Ono[1], Daijiro Konno[2], Takeshi Maeda[3], Seiji Okada[4], Kinichi Nakashima[5], Yasuharu Nakashima[1]

[1]Department of Orthopedic Surgery, Graduate School of Medical Sciences, Kyushu University, Fukuoka, Japan.

[2]Department of Energy and Materials, Faculty of Science and Engineering, Kindai University, Osaka, Japan

[3]Department of Orthopedic Surgery, Spinal Injuries Center, Iizuka, Japan

[4]Department of Orthopedic Surgery, Graduate School of Medical Sciences, Osaka University, Osaka, Japan.

[5]Department of Stem Cell Biology and Medicine, Graduate School of Medical Sciences, Kyushu University, Fukuoka, Japan.

Contact information of all authors

Kazuki Kitade: kitade.kazuki.582@s.kyushu-u.ac.jp

Kazu Kobayakawa: kobayakawa.kazu.000@m.kyushu-u.ac.jp

Hirokazu Saiwai: saiwai.hirokazu.255@m.kyushu-u.ac.jp

Yoshihiro Matsumoto: matsumoto.yoshihiro.540@m.kyushu-u.ac.jp

Kenichi Kawaguchi: kawaguchi.kenichi.241@m.kyushu-u.ac.jp

Keiichiro Iida: iida.keiichiro.979@m.kyushu-u.ac.jp

Ken Kijima: kenkiji68@gmail.com

Hirotaka Iura: hirotaka.iura@gmail.com

Tetsuya Tamaru: 3MD17085E@s.kyushu-u.ac.jp

Yohei Haruta: yohei_haruta@yahoo.co.jp

Gentaro Ono: onokuro@gmail.com

Daijiro Konno: daikon@emat.kindai.ac.jp

Takeshi Maeda: maeken@gd6.so-net.ne.jp

Seiji Okada: seokada@ort.med.osaka-u.ac.jp

Kinichi Nakashima: nakashima.kinichi.718@m.kyushu-u.ac.jp

Yasuharu Nakashima: nakashima.yasuharu.453@m.kyushu-u.ac.jp

***Corresponding author**: Kazu Kobayakawa

e-mail: kobayakawa.kazu.000@m.kyushu-u.ac.jp

address: Department of Orthopedic Surgery, Graduate School of Medical Sciences, Kyushu University, 3-1-1 Higashi-ku, Fukuoka, 812-8582, Japan

Running title

Neonate-specific neuroinflammation after spinal cord injury

Keywords spinal cord injury, neonatal mouse, neuroinflammation, neutrophil, reactive astrocyte

Abstract

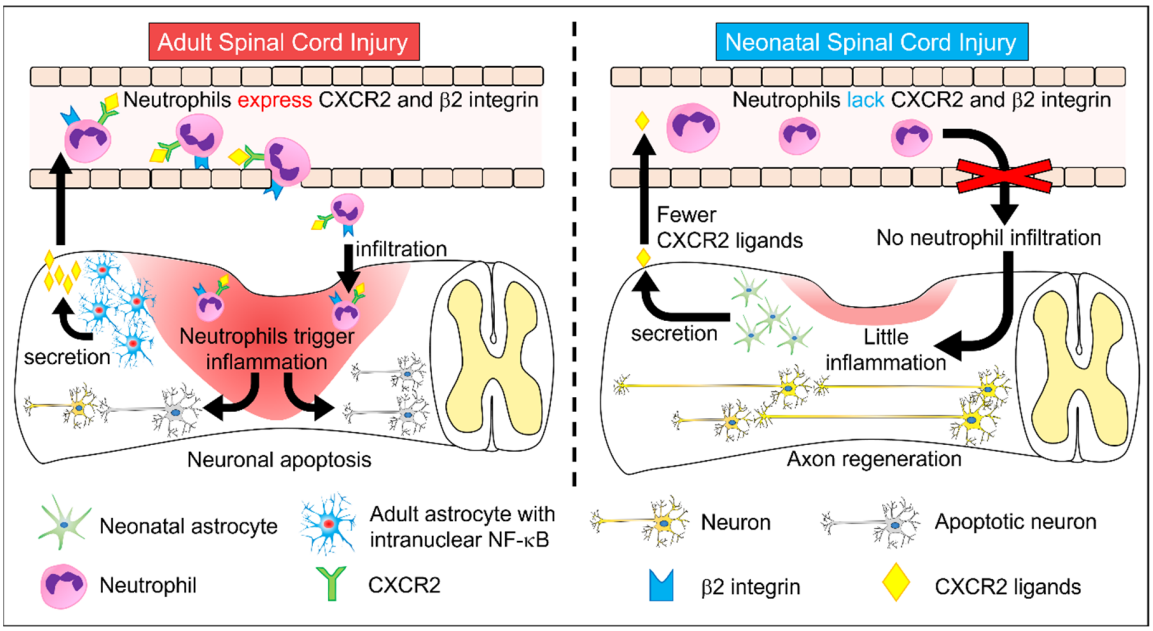

Neonatal spinal cord injury (SCI) shows better functional outcomes than adult SCI. Although the regenerative capability in the neonatal spinal cord may have cues in the treatment of adult SCI, the mechanism underlying neonatal spinal cord regeneration after SCI is unclear. We previously reported age-dependent variation in the pathogenesis of inflammation following SCI. Therefore, we explored differences in the pathogenesis of inflammation after SCI between neonatal and adult mice and their effect on axon regeneration and functional outcome. We established two-day-old spinal cord crush mice as a model of neonatal SCI. Immunohistochemistry of the spinal cord revealed that the nuclear translocation of NF-κB, which promotes the expression of chemokines, was significantly lower in the astrocytes of neonates than in those of adults. Flow cytometry revealed that neonatal astrocytes secrete low levels of chemokines to recruit circulating neutrophils (e.g., *Cxcl1* and *Cxcl2*) after SCI in comparison to adults. We also found that the expression of a chemokine receptor (CXCR2) and an adhesion molecule (β2 integrin) quantified by flow cytometry was lower in neonatal circulating neutrophils than in adult neutrophils. Strikingly, these neonate-specific cellular properties seemed to

be associated with no neutrophil infiltration into the injured spinal cord, followed by significantly lower expression of inflammatory cytokines (*Il-1β*, *Il-6* and *Tnf-α*) after SCI in the spinal cords of neonates than in those of adults. At the same time, significantly fewer apoptotic neurons and greater axonal regeneration were observed in neonates in comparison to adults, which led to a marked recovery of locomotor function. This neonate-specific mechanism of inflammation regulation may have potential therapeutic applications in controlling inflammation after SCI.

Background

The mature mammalian spinal cord does not regenerate once damaged.[1] Therefore, spinal cord injury (SCI) causes permanent motor, sensory, and autonomic nerve damage, which impose physical, psychological, and economic burdens on patients.[2] SCI can occur even in neonates at birth due to head malposition during delivery or the use of suction or forceps for delivery assistance, potentially resulting in quadriplegia.[3] Interestingly, after SCI, neonates often achieve remarkable functional recovery. Through this recovery, even neonates with complete paralysis at the time of injury (i.e., American Spinal Cord Injury Association Impairment Scale A) may regain the ability to walk.[4] This fact suggests that neonates may have greater spinal cord regenerative capacity than adults.

Injury to the spinal cord causes neuroinflammation leading to neuronal apoptosis or demyelination, which worsens the functional prognosis.[5,6] For this reason, suppressing inflammation after SCI is important for improving functional outcomes. However, the inflammatory response following SCI involves complex cellular networks, including several types of blood-derived cells (e.g., neutrophils, monocytes/macrophages, lymphocytes, and mast cells), as well as spinal cord-intrinsic astrocytes and microglia.[6-9]

Considering the inflammatory response at the injured spinal cord caused by blood-derived cells, neutrophils are the first to infiltrate into the injured spinal cord as the main initiator of a complex inflammatory cascade,[10,11] suggesting that the suppression of neutrophil infiltration would be quite effective for inflammation control. In addition to infiltrating blood-derived inflammatory cells, astrocytes also contribute to enhancing the inflammatory response at the injured spinal cord, secreting the neutrophil attractant chemokine CXCL1.[12] Therefore, elucidation of the cellular properties of both neutrophils and astrocytes in the injured spinal cord is important for controlling acute phase inflammation after SCI.[13,14]

Neutrophils and astrocytes in the injured spinal cord also affect axon regeneration. When

inflammatory cytokines secreted from infiltrated neutrophils act on astrocytes, naïve astrocytes are activated and phenotypically changed to become reactive astrocytes. Reactive astrocytes then form glial scars that physically and chemically inhibit axon regeneration.[14-16] Once formed, the glial scar remains until the chronic phase of SCI;[17] thus, the suppression of astrocyte activation is important for preventing glial scar formation. To address this problem of astrocyte interference in axon regeneration, the neutrophil-astrocyte interaction in the injured spinal cord should be elucidated. However, how neutrophils interact with astrocytes in neonates after SCI is unclear, whereas neonates regain better locomotor function after SCI than adults.

Here, we established a spinal cord crush injury model using postnatal day 2 (P2) mice and adult mice to investigate the spinal cord regenerative capacity and pathophysiology in the acute phase of SCI, focusing on neuroinflammation due to astrocytes and neutrophils, axon regeneration and gait functions. Cell sorting from the injured spinal cord and gene expression analysis revealed a different pattern of inflammatory cell infiltration between adults and neonates. The neonate-specific inflammatory cell infiltration patterns were related to chemokine-chemokine receptor interaction properties between astrocytes and neutrophils. Furthermore, we found a difference in the neutrophil adhesion molecule expression states that was also associated with neonate-specific inflammatory responses. Neonatal spinal cord regeneration seemed to be associated with neonate-specific inflammation regulatory mechanisms.

Materials and Methods

Mice

Wild-type C57/BL6N mice (Japan SLC, Japan) and Aldh1l1-EGFP transgenic mice were used in the study. Postnatal day 2 pups (P2) and 8-week-old mice were used as neonatal and adult mice, respectively. A total of 156 mice were randomly assigned to the sham group or the SCI group with

matching for age. Randomization was performed using computer-generated random numbers. All mice were housed with humidity controlled to 30–70%, temperature controlled to 21–23°C, and a 12-hour light-dark cycle. All experimental procedures were conducted in compliance with animal protocols approved by the Committee of Ethics on Animal Experimentation in the Faculty on Medicine, Kyushu University (A22-238-0). All measurements were performed with the experimenter blinded to group identity.

Spinal cord crush injury

Mice were anesthetized with isoflurane inhalation (4% induction, 3% maintenance). A 5 mm skin incision was made along the sagittal midline of the spine, and laminectomy of the T9 laminae was performed to expose and crush the spinal cord at the T10 spinal segment. The spinal cord was fully compressed for 2 seconds with forceps (width: 100 μm). The tips of the forceps were continuously attached on the back wall of the vertebrae during the crush procedure. After crush injury, the skin was closed with 6-0 nylon thread. Meloxicam (0.2 mg/kg) was administered subcutaneously for analgesia and placed into a temperature-controlled chamber during recovery from anesthesia to regain thermoregulation. Sham-operated controls were also anesthetized with isoflurane and subjected to laminectomy only. We confirmed that the dura mater was not affected by crush injury in either adults or neonates (Supplementary figure S1).

Analysis of the locomotor function

Open field locomotor function was evaluated via the Basso Mouse Scale scoring system at 7, 14, 28, and 112 days after injury.[18] A footprint analysis was performed as previously described.[19] Briefly, the forelimbs and hindlimbs were dipped in red and green dyes, respectively. The mice walked on a paper-covered runway 4 cm in width and 80 cm in length. A bright box was placed at the beginning of the

runway, and a dark box was also placed with food at the end of the runway.

Flow cytometry

At 12 hours after crush injury, animals were reanesthetized with a lethal dose of isoflurane and perfused with ice-cold normal saline for circulating blood removal. A spinal cord specimen (6 mm in length) centered on the epicenter of the lesion was rapidly dissected from the vertebral column and placed into type 1 collagenase solution (100 U/ml; Invitrogen). The spinal cord was minced using scissors and incubated in the solution for 25 minutes at 37°C for gradual dissociation. Dissociated cells were centrifuged at 4000 rpm for 1 minute, suspended in Dulbecco's modified Eagle's medium containing 10% fetal bovine serum and passed through a 40 μm nylon strainer. For blood sample collection, cardiac puncture was conducted on mice at 12 hours after crush injury. After removing red blood cells by BD Pharm Lyse (BD Biosciences, San Jose, CA), the resulting suspension was centrifuged and washed twice in FACS buffer. These suspensions were pelleted by centrifugation and incubated at 4°C for 30 minutes with the following fluorescent antibodies: phycoerythrin-Cy7-conjugated CD45, fluorescein isothiocyanate-conjugated Gr-1, allophycocyanin-conjugated CD11b, phycoerythrin-conjugated CXCR2, and phycoerythrin-conjugated β2 integrin (BioLegend, San Diego, CA). Before the analysis, 7-amino-actinomycin D (BD Biosciences) was added to determine the cell viability. All samples were suspended in 500 μl of FACS buffer and analyzed using a FACSfusion flow cytometer (BD Biosciences). The data were analyzed using the FACSDiva software program (BD Biosciences).

Quantitative real-time PCR

Total RNA was isolated from each injured spinal cord specimen (length: 6 mm; centered on the epicenter of the lesion) using an RNeasy Mini Kit (Qiagen, Hilden, Germany). RNA was reverse

transcribed using PrimeScript Reverse Transcriptase (TaKaRa, Shiga, Japan). Quantitative real-time PCR was conducted on 20 μl of reaction mixture with primers specific to the genes of interest (Table 1) and TB Green Premix DimmerEraser (TaKaRa). mRNA levels in each sample were normalized to those of glyceraldehyde-3-phosphate dehydrogenase. For the mRNA expression analysis of neutrophils and astrocytes, these cells were individually isolated from the spinal cord via FACSfusion, and total RNA isolation was performed using the RNeasy Micro Kit (Qiagen).

Immunohistochemistry

Mice were reanesthetized and transcardially perfused with ice-cold normal saline, followed by fixation with 4% paraformaldehyde. The spinal cord was removed and immersed in the same fixative for 24 hours. The spinal cord was dehydrated in 10% sucrose solution for 1 hour and subsequently in 30% sucrose solution for 24 hours. The spinal cord was embedded in an optimal cutting temperature compound. Frozen sections were cut on a cryostat in the sagittal plane at 16 μm. The sections were stained with primary antibodies at 4°C overnight, followed by a 1-hour incubation with fluorescence-conjugated secondary antibodies and Hoechst 33342 (1:1000; Invitrogen). The applied primary antibodies were as follows: Ly6B.2 (rat, MCA771GA; 1:400; BIO RAD), GFAP (rat, no.13-0300; 1:400; Invitrogen), NF-κB p65 (rabbit, sc-372: 1:400; Santa Cruz Biotechnology), NeuN (mouse, MAB377; 1:400; Sigma–Aldrich), cleaved caspase-3 (rabbit, no.9579T; 1:400; Cell Signaling Technology), and 5-HT (goat, no.20079; 1:400; ImmunoStar). For the evaluation of apoptotic cells in the injured spinal cord, a terminal deoxynucleotidyl transferase-mediated dUTP nick-end labeling (TUNEL) assay was performed using an ApopTag red in situ kit (Chemicon, Temecula, CA).

Quantitative analysis for immunohistology

For the quantification of $Ly6B.2^+$ neutrophils, intranuclear $p65^+/GFAP^+$ cells, $TUNEL^+$ cells, cleaved

caspase-3^+/$NeuN^+$ cells, and $NeuN^+$ cells in the spinal cord at 12 hours after injury, 10-mm-long sagittal sections at 200-μm intervals were viewed on a light microscope (BZ-9000; Keyence, Osaka, Japan), and each cell was counted using the Dynamic Cell Count BZ-H1C software program (Keyence). The numbers of 5-HT^+ areas per 1 mm^2 segment were calculated using ImageJ (National Institutes of Health). For the comparison of astrocyte process lengths of adult and neonatal pups at 12 hours after injury, 20 astrocytes were randomly selected per field of view in each section, and the average length of the longest projection of each astrocyte was calculated.

Statistical analysis

Statistical analyses to compare the means of data between two groups were performed using unpaired *t* tests. For analyses of the repeated measures and multiple group comparisons, a two-way repeated-measures ANOVA with the Tukey–Kramer post-hoc test was performed. All tests were two-tailed, and *P* values of < 0.05 were considered statistically significant. Data in the graphs are presented as the mean ± SEM. All analyses were conducted using the JMP PRO 16.0.0 software program (SAS Institute, Cary, NC, USA). We performed a post-hoc power analysis to confirm that each analysis had sufficient statistical power (Table 2).

Results

The expression of inflammatory cytokines and chemokines in the acute phase of SCI is lower in neonates than in adults

We have previously reported that inflammation after SCI is milder in young mice than in adult mice.[20] Therefore, we hypothesized that the pathophysiology of neuroinflammation after SCI changes in an age-dependent manner and investigated whether there is a difference in the inflammatory response after SCI between adults and neonates. The gene expression analysis of the

spinal cord at 12 hours after injury, when the expression of inflammatory cytokines peaks,[20] revealed that there was a statistically significant interaction between the effects of mouse age and crush injury on the expression levels of *Il-1β* ($F(1, 28) = 38.85$, $P<0.0001$), *Il-6* ($F(1, 28) = 12.24$, $P=0.0016$) and *Tnf-α* ($F(1, 28) = 51.00$, $P<0.0001$). The simple main effects analysis showed that the expression levels of *Il-1β, Il-6* and *Tnf-α* in neonates after SCI were significantly lower than those in adults ($P<0.0001$, = 0.0002, and < 0.0001, respectively), whereas no significant differences were found in the spinal cord of sham-operated neonates and adults ($P>0.9999$, $P>0.9999$, and $P=0.9890$, respectively) (Fig. 1A). The expression of these inflammatory cytokines is associated with the infiltration of inflammatory cells, such as neutrophils and monocytic cells, which migrate toward chemotactic factors.[21] Therefore, we examined the expression level of several chemokines in the spinal cord at 12 hours after injury and found a statistically significant interaction between the effects of mouse age and crush injury on the expression levels of *Cxcl1* ($F(1, 28) = 16.54$, $P=0.0004$), *Cxcl2* ($F(1, 28) = 11.08$, $P=0.0024$), *Cxcl5* ($F(1, 28) = 37.85$, $P<0.0001$), *Ccl2* ($F(1, 28) = 19.80$, $P=0.0001$), and *Ccl3* ($F(1, 28) = 41.32$, $P<0.0001$), which promoted the migration of neutrophils and macrophages. The simple main effects analysis showed that the expression levels of *Cxcl1*, *Cxcl2*, *Cxcl5*, *Ccl2*, and *Ccl3* in neonates after SCI were significantly lower than those in adults ($P<0.0001$, $P=0.0003$, $P<0.0001$, $P<0.0001$, and $P<0.0001$, respectively), whereas no significant differences were found in the spinal cord of sham-operated neonates and adults ($P>0.9999$, $P>0.9999$, $P>0.9999$, $P>0.9999$, and $P=0.9975$, respectively) (Fig. 1B).

Few neutrophils infiltrate the injured spinal cord in neonatal mice

Neonatal spinal cord specimens showed lower chemokine levels than adult spinal cord specimens at 12 hours after SCI. This difference may have affected the number of infiltrating neutrophils or macrophages that migrate under the influence of chemokines. Therefore, the numbers of

inflammatory cells infiltrating into the spinal cord at 12 hours after injury were investigated by flow cytometry. In adults, both monocytic cells ($CD45^{posi}/CD11b^{posi}/Gr\text{-}1^{nega\text{-}int}$) and neutrophils ($CD45^{posi}/CD11b^{posi}/Gr\text{-}1^{high}$) infiltrated the spinal cord at 12 hours after injury. Surprisingly, the neonatal spinal cord had no neutrophil infiltration at 12 hours after injury in contrast to the adult spinal cord (t=3.495, df=8, P=0.0081, two-tailed), whereas neutrophils were present in the peripheral blood (Fig. 2A, 2B). Furthermore, immunostaining showed that $Ly6B.2^{+}$ neutrophils infiltrated into the adult spinal cord at 12 hours after injury, but not into the neonatal spinal cord (t=7.841, df=8, P<0.0001, two-tailed), similar to the flow cytometry results (Fig. 2C, D).

Astrocyte-derived neutrophil chemokine expression in neonates is lower than that in adults after SCI

We showed that the expression levels of several chemokines in the injured spinal cord of neonates were lower than those in adults and that neutrophils did not eventually infiltrate the spinal cord. It is still unclear why the expression of neutrophil migration factor is low in neonates. Since astrocytes secrete chemokines in mammalian CNS injury and promote the infiltration of neutrophils beyond the blood–brain barrier into the CNS,[12,22-24] we decided to compare astrocyte-derived chemokine expression between adults and neonates. Using Aldh1l1-EGFP transgenic mice, a reporter mouse for astrocytes (Fig. 3A), $EGFP^{+}$ astrocytes were collected by flow cytometry (Fig. 3B). The gene expression analysis of $EGFP^{+}$ astrocytes at 12 hours after SCI revealed that there was a statistically significant interaction between the effects of mouse age and crush injury on the expression levels of *Cxcl1* (F(1, 20) = 8.817, P=0.0096) and *Cxcl2* (F(1, 20) = 13.23, P=0.0016), both of which are neutrophil migration factors. [12,21,25,26] The simple main effects analysis showed that the expression levels of *Cxcl1* and *Cxcl2* in neonatal astrocytes after SCI were significantly lower than those in adults (P=0.0033 and 0.0003, respectively), whereas no significant differences were found in the astrocytes

of sham-operated neonates and adults (P>0.9999, respectively) (Fig. 3C). The expression of *Cxcl1* and *Cxcl2* from spinal cord astrocytes is regulated by p65, a transcription factor of the NF-κB family.[23,27] The comparison of p65 expression in astrocytes by immunostaining revealed a significant decrease in the intranuclear translocation of p65 in astrocytes of neonates compared to that of adults (t=6.399, df=8, P=0.0002, two-tailed) (Fig. 3D – 3F). Interestingly, adult astrocytes colocalized with p65 showed reactive astrocyte-like morphology with significantly elongated processes in comparison to astrocytes from neonates (t=14.59, df=8, P<0.0001, two-tailed) (Fig. 3G).

Circulating neutrophils express fewer chemokine receptors and adhesion molecules in neonates than in adults

Since neutrophil migration and infiltration are tightly controlled by interactions between chemokines and chemokine receptors, as well as adhesion molecules and the endothelium,[28,29] the lack of neutrophil infiltration in the injured spinal cord in neonates may also be related to these neutrophil surface antigen expression levels. We used flow cytometry to quantify CXCR2 (a receptor for CXCL1 and CXCL2)[28] and β2 integrin (an adhesion molecule required for neutrophil infiltration outside of blood vessels)[30,31] in neonatal circulating neutrophils. As a result, the level of CXCR2 in circulating neutrophils of neonates was significantly lower than that of adults (t=6.452, df=8, P=0.0002, two-tailed) (Fig. 4A, 4B). Furthermore, β2 integrin expression in neonatal circulating neutrophils was significantly lower than that in adult circulating neutrophils (t=13.67, df=8, P<0.0001, two-tailed). (Fig. 4C, 4D).

Secondary injury after SCI is attenuated in neonatal mice

The inflammatory responses after SCI cause neuronal apoptosis and demyelination (called secondary injury) and significantly affect the functional outcome.[5,6,8] Since the acute inflammatory response

differs between neonatal and adult mice, we decided to compare the magnitude of secondary injury between the two groups by performing TUNEL staining, which reflects apoptosis throughout the spinal cord (Fig. 5A). As a result, there was a statistically significant interaction between the effects of mouse age and crush injury on the number of TUNEL-positive apoptotic cells ($F(1, 16) = 35.05$, $P<0.0001$). The simple main effects analysis showed that the number of TUNEL-positive apoptotic cells in the neonatal spinal cord after SCI was significantly lower than that in adults ($P<0.0001$), whereas no significant differences were found in the spinal cord of sham-operated neonates and adults ($P=0.9763$) (Fig. 5B, 5C). We subsequently investigated whether apoptosis was induced by the extrinsic pathway because TNF-α causes caspase-3-mediated apoptosis of neurons and oligodendrocytes.[6] Immunostaining revealed a greater number of intranuclear translocated cleaved caspase-3 proteins colocalized with neurons in adults than in neonates ($t=9.297$, df=8, $P<0.0001$, two-tailed) (Fig. 5D, 5E), suggesting that neuronal apoptosis induced by the extrinsic pathway is less likely to occur in neonates after SCI. As a result of attenuated neuronal apoptosis, the number of neurons on day 3 after injury was significantly higher in the neonates than in the adults ($F(2, 30) = 4.286$, $P=0.0230$) at the epicenter of the lesion ($P<0.0001$) in addition to the rostral side ($P<0.0001$) and caudal side ($P<0.0001$) of the lesion (Fig. 5F).

Axon regeneration and good recovery of motor function in neonatal mice after SCI

Because IL-1β in the injured spinal cord has been reported to exacerbate axon regeneration,[32] we decided to examine the effects of the different inflammatory cytokine expression levels between adults and neonates on axon regeneration. Immunostaining revealed that 5-HT$^+$ axons disappeared caudal to the injured area on day 3 after SCI in both adults and neonates (Fig. 6A). However, 5-HT$^+$ axons were vigorously extended on the caudal side of the injured area in neonates at 2 weeks after injury, whereas little recovery was observed in adults (Fig. 6A). Consequently, the number of 5-HT$^+$

axons on the caudal side of the injured area was significantly greater in neonates than in adults (t=6.929, df=8, P<0.0001, two-tailed) (Fig. 6B). Locomotor function, as assessed by the BMS, which is related to the magnitude of regenerated 5-HT$^+$ axons,[33,34] was significantly better in neonates than in adults (F(6, 60) = 9.397, P<0.0001: Tukey–Kramer post hoc test, P<0.0001) (Fig. 6C). The footprint analysis showed that adult mice walked with their green pigmented hindlimbs dragging, while neonate hindlimbs and forelimbs were placed in coordination (Fig. 6D). The footprint analysis also revealed that the hindlimb rotation of neonates was improved, while adult mice suffered residual rotation (t=43.10, df=8, P<0.0001, two-tailed) (Fig. 6E).

Discussion

In this study, we discovered that the expression levels of intranuclear NF-κB and associated chemokines in the astrocytes of neonatal mice were significantly lower than those in adult mice after SCI. Moreover, the expression levels of chemokine receptors and adhesion molecules in the neutrophils in neonatal mice were markedly lower than those in adult mice. These neonate-specific cellular properties were accompanied by no neutrophil infiltration into the spinal cord and little inflammation, mild secondary injury, and remarkable spinal cord repair with good recovery of locomotor functions after SCI. In regard to the functional properties of circulating neutrophils in neonates, the expression levels of both CXCR2 and β2 integrin at 12 hours after injury were significantly lower than those in adults (Fig. 4A-4D). In a study using neutrophil-specific CXCR2-depleted adult mice with experimental autoimmune encephalomyelitis, the infiltration of neutrophils into the spinal cord was observed.[35] From this result, the neutrophil-free inflammation seen in this study could not be solely caused by the reduced expression of CXCR2. β2 Integrin combined with CD11a and CD11b forms the adhesion molecules LFA-1 and MAC-1, respectively.[36-38] LFA-1 and MAC-1 play roles in stopping on, crawling on, and transmigrating through vessel walls in the series

of neutrophil migration.[37,38] Thus, the low expression of β2 integrin has a negative effect on several steps of neutrophil infiltration into the spinal cord. Taken together, the neutrophil-free inflammation in the neonates of this study was due to the simultaneous lower expression of CXCR2 and β2 integrin. This fact suggests that combined inhibition of CXCR2 and β2 integrin can be considered to suppress post-SCI inflammation in adults as much as in neonates. To date, no study has evaluated the properties of neutrophils in neonates after SCI in comparison to adults. Through a comprehensive understanding of the age-dependent differences in the functional properties of neutrophils, we may be able to achieve neonatal-like reduced inflammation and vigorous axon regeneration with favorable functional recovery, even in the adult spinal cord.

Spinal cord regeneration in mature mammals has never been reported. However, in opossums soon after birth, spinal cord regeneration after injury has been observed, although they belong to a mammalian class.[39] It has also been reported that in neonatal mice with SCI, the spinal cord is histologically repaired following microglia-mediated fibronectin secretion.[40] These facts suggest that the mammalian spinal cord has regenerative potential soon after birth. In the present study, we have advanced the research on this topic by confirming that neonatal mice with SCI demonstrate axon regeneration in the context of extremely low inflammation that is characterized by a lack of neutrophil infiltration. Furthermore, we proved that neutrophil-free inflammation in neonates results from the lower expression of chemokines from astrocytes and the lower expression of chemokine receptors and adhesion molecules on neutrophils in comparison to adults. In a study using young (age: 4 weeks) mice with SCI, fewer neutrophils infiltrated into the injured spinal cord of young mice in comparison to adult mice.[20] It has also been reported that when IL-1β was administered to the brain parenchyma of rodents of varying ages, the vascular permeability and the number of infiltrating neutrophils differed according to the maturity of the animals, indicating that the sensitivity to IL-1β depends on age.[41] These facts, coupled with our results, suggest that aging is

a factor that affects the amount of neutrophil infiltration after SCI. Astrocytes may be related to the age-dependent change in neutrophil migration. Since the astrocyte nuclear NF-κB binding capacity in the brain changes in an age-dependent manner,[42] NF-κB-mediated chemokine release from astrocytes and neutrophil infiltration after SCI may be affected by aging. Taken together, elucidation of the age-dependent pathophysiology of inflammation after SCI is important for optimal inflammation control and the effective prevention of secondary injury. Considering the fact that neutrophil infiltration has been observed—to some extent—after CNS injury in 9- and 10-day-old mice,[10,43] the 2-day-old mice with SCI used in this study are an extremely optimal model for analyzing the mechanisms of successful suppression of neutrophil infiltration and subsequent inflammation.

Although astrocytes induce neutrophil infiltration through NF-κB-mediated chemokine release after CNS injury,[12,23,27] the functional state of NF-κB in neonatal astrocytes after SCI had remained unclear. Our study revealed that NF-κB nuclear translocation and the resulting chemokine release after SCI were milder in neonatal astrocytes. Interestingly, the nuclear translocation of NF-κB in adult astrocytes was accompanied by morphological changes, such as hypertrophy and process elongation, indicating a reactive astrocyte phenotype.[14] This NF-κB-mediated morphological change in astrocytes has also been observed in damaged brain white matter of a mouse model of vascular dementia, where astrocytes with transgenic NF-κB inhibition did not show the reactive astrocyte phenotype.[44] In addition, the gene expression profile of reactive astrocytes in LPS-stimulated brain or hypoxia-damaged brain contains higher NF-κB levels in comparison to naïve astrocytes.[45] Thus, NF-κB in astrocytes after CNS injury has a dual role in the activation of astrocytes and the expression of chemokines. When naïve astrocytes become reactive astrocytes, they form a glial scar through interaction with type 1 collagen in the injured spinal cord,[14] whereas astrocytes before activation do not interact with type 1 collagen. For this reason, the inhibition of astrocyte activation is important to

prevent glial scar formation.[14] Furthermore, mice with selective transgenic inhibition of astrocyte NF-κB show reduced lesion volumes and a reduction in chondroitin sulfate proteoglycans, which participate in glial scar formation.[46] These facts suggest that NF-κB signaling in astrocytes is the optimal therapeutic target for the prevention of glial scar formation following astrocyte activation, as well as neutrophil infiltration by chemokine secretion. Accordingly, reproduction of neonate-like inflammatory regulation in adult SCI may be beneficial for preventing glial scar formation as well as secondary injury after SCI.

The present study was associated with several limitations. First, we did not examine the effect of sex differences on the results of the study because it is often difficult to determine the sex of mice on postnatal day 2. Second, while we showed a correlation between juvenile astrocytes and spinal cord repair in neonatal mice, we did not show direct causality. To confirm their direct causality, a method to juvenilize astrocytes in the adult spinal cord or to make astrocytes in neonatal mice senescent might be established.

Conclusion

Astrocytes in neonatal mice after SCI show low activation and release low levels of NF-κB-mediated chemokines, such as CXCL1 and CXCL2. In addition, in neonatal neutrophils, the expression of the chemokine receptor CXCR2 and the adhesion molecule β2 integrin is lower than that in adult neutrophils. These neonatal specific cellular properties were correlate with a neutrophil-free inflammatory response with the reduced expression of inflammatory cytokines (e.g., IL-6, IL-1β, and TNF-α) after SCI accompanied with attenuated secondary injury and remarkable spinal cord regeneration. Our findings provide deeper insight into the role of astrocytes and neutrophils in neuroinflammation and axon regeneration, highlighting the importance of a neonate-like neutrophil-free inflammatory response after traumatic spinal cord injury.

Transparency, Rigor, and Reproducibility Summary

Five to eight mice per group were used to detect both an overall significant effect of the repeated-measures ANOVA (the primary statistical analysis) and a post hoc difference between the best performing experimental group vs. control with $p < 0.05$ after correction for multiple comparisons. Overall, 173 mice were subjected to experimental injury, including neonates and adults. Five were excluded for technical reasons, and 12 neonates died after SCI. Complete data were obtained from 156 mice. Both neonates and adults were randomly assigned to the naïve group or SCI group by using a random number generator.

Abbreviations

5-HT: 5-hydroxytryptamine; Aldh1l1: aldehyde dehydrogenase 1 family member L1; BMS: Basso Mouse Scale; CCL: C-C motif chemokine ligand; CNS: central nervous system; CXCL: C-X-C motif chemokine ligand; CXCR: C-X-C chemokine receptor; dUTP: deoxyuridine triphosphate; EGFP: enhanced green fluorescent protein; IL: interleukin; Gapdh: glyceraldehyde-3-phosphate dehydrogenase; GFAP: glial fibrillary acid protein; LFA-1: lymphocyte function-associated antigen 1; LPS: lipopolysaccharide; MAC-1: macrophage-1 antigen; NF-kB: nuclear factor kappa B; TNFα: tumor necrosis factor alpha; SCI: spinal cord injury; TUNEL: terminal deoxynucleotidyl transferase-mediated dUTP nick-end labeling

Ethics approval

All surgical procedures and experimental manipulations were approved by the Committee of Ethics on Animal Experimentation in the Faculty on Medicine, Kyushu University (A-22-238-0). Experiments were conducted under the control of the Guidelines for Animal Experimentation.

Consent for publication

Not applicable.

Availability of data and materials

All data generated or analyzed during this study are included in this published article.

Acknowledgments

Aldh1l1-EGFP transgenic mice were kindly provided by Y. Gotoh (Tokyo University, Tokyo, Japan). We thank The Research Support Center, Research Center for Human Disease Modeling, Kyushu University Graduate School of Medical Sciences for technical assistance regarding flow cytometry. We are also grateful to J. Kishimoto (Center for Clinical and Translational Research, Kyushu University Hospital) for supervision of the statistical analyses.

Author's contributions

K. Kitade: Conceptualization (lead); investigation; formal analysis; writing – original draft (lead). K. Kobayakawa and H. Saiwai: Supervision; funding acquisition; writing – original draft (supporting). K. Kijima, H. Iura, T. Tamaru, Y. Haruta, and G. Ono: Conceptualization (supporting); writing – review and editing (equal). Other authors: Writing – review and editing (equal).

Competing interests

The authors have no competing interests to disclose.

Funding

This work was supported by JSPS KAKENHI Grant Number JP22K19587, JP22K09426, and

JP22H03200; The General Insurance Association of Japan; ZENKYOREN (National Mutual Insurance Federation of Agricultural Cooperatives). The funders had no role in the study design, data collection, data analyses, interpretation, or writing of the manuscript.

References

1. Sofroniew MV. Dissecting spinal cord regeneration. Nature 2018 May;557(7705):343-350; doi: 10.1038/s41586-018-0068-4.

2. McDonald JW, Sadowsky C. Spinal-cord injury. Lancet 2002 Feb 2;359(9304):417-25; doi: 10.1016/S0140-6736(02)07603-1.

3. Vialle R, Piétin-Vialle C, Ilharreborde B, et al. Spinal cord injuries at birth: a multicenter review of nine cases. J Matern Fetal Neonatal Med 2007 Jun;20(6):435-40; doi: 10.1080/14767050701288325.

4. Wang MY, Hoh DJ, Leary SP, et al. High rates of neurological improvement following severe traumatic pediatric spinal cord injury. Spine 2004 Jul 1;29(13):1493-7; doi: 10.1097/01.brs.0000129026.03194.0f.

5. Saiwai H, Ohkawa Y, Yamada H, et al. The LTB4-BLT1 axis mediates neutrophil infiltration and secondary injury in experimental spinal cord injury. Am J Pathol 2010 May;176(5):2352-66; doi: 10.2353/ajpath.2010.090839.

6. Kobayakawa K, Kumamaru H, Saiwai H, et al. Acute hyperglycemia impairs functional improvement after spinal cord injury in mice and humans. Sci Transl Med 2014 Oct 1;6(256):256ra137; doi: 10.1126/scitranslmed.3009430.

7. Kobayakawa K, Ohkawa Y, Yoshizaki S, et al. Macrophage centripetal migration drives spontaneous healing process after spinal cord injury. Sci Adv 2019 May 15;5(5):eaav5086; doi: 10.1126/sciadv.aav5086.

8. Yoshizaki S, Kijima K, Hara M, et al. Tranexamic acid reduces heme cytotoxicity via the TLR4/TNF axis and ameliorates functional recovery after spinal cord injury. J Neuroinflammation 2019 Jul 29;16(1):160; doi: 10.1186/s12974-019-1536-y.

9. Zhang C, Yan Z, Maknojia A, et al. Inhibition of astrocyte hemichannel improves recovery from spinal cord injury. JCI Insight 2021 Mar 8;6(5):e134611; doi: 10.1172/jci.insight.134611.

10. Yao HW, Kuan CY. Early neutrophil infiltration is critical for inflammation-sensitized hypoxic-ischemic brain injury in newborns. J Cereb Blood Flow Metab 2020 Nov;40(11):2188-2200; doi: 10.1177/0271678X19891839.

11. Pang QM, Chen SY, Xu QJ, et al. Neuroinflammation and Scarring After Spinal Cord Injury: Therapeutic Roles of MSCs on Inflammation and Glial Scar. Front Immunol 2021 Dec 2;12:751021; doi: 10.3389/fimmu.2021.751021.

12. Michael BD, Bricio-Moreno L, Sorensen EW, et al. Astrocyte- and Neuron-Derived CXCL1 Drives Neutrophil Transmigration and Blood–Brain Barrier Permeability in Viral Encephalitis. Cell Rep 2020 Sep 15;32(11):108150; doi: 10.1016/j.celrep.2020.108150.

13. Sofroniew MV. Astrocyte Reactivity: Subtypes, States, and Functions in CNS Innate Immunity. Trends Immunol 2020 Sep;41(9):758-770; doi: 10.1016/j.it.2020.07.004.

14. Hara M, Kobayakawa K, Ohkawa Y, et al. Interaction of reactive astrocytes with type I collagen induces astrocytic scar formation through the integrin-N-cadherin pathway after spinal cord injury. Nat Med 2017 Jul;23(7):818-828; doi: 10.1038/nm.4354.

15. Okada S, Hara M, Kobayakawa K, et al. Astrocyte reactivity and astrogliosis after spinal cord injury. Neurosci Res 2018 Jan;126:39-43; doi: 10.1016/j.neures.2017.10.004.

16. Okada S, Nakamura M, Katoh H, et al. Conditional ablation of Stat3 or Socs3 discloses a dual role for reactive astrocytes after spinal cord injury. Nat Med 2006 Jul;12(7):829-34; doi: 10.1038/nm1425.

17. Silver J, Miller JH. Regeneration beyond the glial scar. Nat Rev Neurosci 2004 Feb;5(2):146-56; doi: 10.1038/nrn1326.

18. Basso DM, Fisher LC, Anderson AJ, et al. Basso Mouse Scale for locomotion detects differences in recovery after spinal cord injury in five common mouse strains. J Neurotrauma 2006 May;23(5):635-59; doi: 10.1089/neu.2006.23.635.

19. Yokota K, Kobayakawa K, Saito T, et al. Periostin Promotes Scar Formation through the Interaction between Pericytes and Infiltrating Monocytes/Macrophages after Spinal Cord Injury. Am J Pathol 2017 Mar;187(3):639-653; doi: 10.1016/j.ajpath.2016.11.010.

20. Kumamaru H, Ohkawa Y, Saiwai H, et al. Direct isolation and RNA-seq reveal environment-dependent properties of engrafted neural stem/progenitor cells. Nat Commun 2012;3:1140; doi: 10.1038/ncomms2132.

21. Pelisch N, Rosas Almanza J, Stehlik KE, et al. CCL3 contributes to secondary damage after spinal cord injury. J Neuroinflammation 2020 Nov 27;17(1):362; doi: 10.1186/s12974-020-02037-3.

22. Zhang P, Liu X, Zhu Y, et al. Honokiol inhibits the inflammatory reaction during cerebral ischemia reperfusion by suppressing NF-κB activation and cytokine production of glial cells. Neurosci Lett 2013 Feb 8;534:123-7; doi: 10.1016/j.neulet.2012.11.052.

23. Choi SS, Lee HJ, Lim I, et al. Human astrocytes: secretome profiles of cytokines and chemokines. PLoS One 2014 Apr 1;9(4):e92325; doi: 10.1371/journal.pone.0092325.

24. Zhou Y, Guo W, Zhu Z, et al. Macrophage migration inhibitory factor facilitates production of CCL5 in astrocytes following rat spinal cord injury. J Neuroinflammation 2018 Sep 4;15(1):253; doi: 10.1186/s12974-018-1297-z.

25. Pineau I, Sun L, Bastien D, et al. Astrocytes initiate inflammation in the injured mouse spinal cord by promoting the entry of neutrophils and inflammatory monocytes in an IL-1 receptor/MyD88-dependent fashion. Brain Behav Immun 2010 May;24(4):540-53; doi: 10.1016/j.bbi.2009.11.007.

26. Hellenbrand DJ, Quinn CM, Piper ZJ, et al. Inflammation after spinal cord injury: a review of the critical timeline of signaling cues and cellular infiltration. J Neuroinflammation 2021 Dec 7;18(1):284; doi: 10.1186/s12974-021-02337-2.

27. Xu J, Zhu MD, Zhang X, et al. NFκB-mediated CXCL1 production in spinal cord astrocytes contributes to the maintenance of bone cancer pain in mice. J Neuroinflammation 2014 Mar 1;11:38; doi: 10.1186/1742-2094-11-38.

28. Eash KJ, Greenbaum AM, Gopalan PK, et al. CXCR2 and CXCR4 antagonistically regulate neutrophil trafficking from murine bone marrow. J Clin Invest 2010 Jul;120(7):2423-31; doi: 10.1172/JCI41649.

29. Ley K, Laudanna C, Cybulsky MI, et al. Getting to the site of inflammation: the leukocyte adhesion cascade updated. Nat Rev Immunol 2007 Sep;7(9):678-89; doi: 10.1038/nri2156.

30. Ou Z, Dolmatova E, Lassègue B, et al. β1- and β2-integrins: central players in regulating vascular permeability and leukocyte recruitment during acute inflammation. Am J Physiol Heart Circ Physiol 2021 Feb 1;320(2):H734-H739; doi: 10.1152/ajpheart.00518.2020.

31. Mabon PJ, Weaver LC, Dekaban GA. Inhibition of monocyte/macrophage migration to a spinal cord injury site by an antibody to the integrin alphaD: a potential new anti-inflammatory treatment. Exp Neurol 2000 Nov;166(1):52-64; doi: 10.1006/exnr.2000.7488.

32. Boato F, Rosenberger K, Nelissen S, et al. Absence of IL-1β positively affects neurological outcome, lesion development and axonal plasticity after spinal cord injury. J Neuroinflammation 2013 Jan 14;10:6; doi: 10.1186/1742-2094-10-6.

33. Musienko P, van den Brand R, Märzendorfer O, et al. Controlling specific locomotor behaviors through multidimensional monoaminergic modulation of spinal circuitries. J Neurosci 2011 Jun 22;31(25):9264-78; doi: 10.1523/JNEUROSCI.5796-10.2011.

34. Perrin FE, Noristani HN. Serotonergic mechanisms in spinal cord injury. Exp Neurol 2019

Aug;318:174-191; doi: 10.1016/j.expneurol.2019.05.007.

35. Khaw YM, Cunningham C, Tierney A, et al. Neutrophil-selective deletion of Cxcr2 protects against CNS neurodegeneration in a mouse model of multiple sclerosis. J Neuroinflammation 2020 Feb 4;17(1):49; doi: 10.1186/s12974-020-1730-y.

36. Anderson DC, Rothlein R, Marlin SD, et al. Impaired transendothelial migration by neonatal neutrophils: abnormalities of Mac-1 (CD11b/CD18)-dependent adherence reactions. Blood 1990 Dec 15;76(12):2613-21.

37. Hyun YM, Choe YH, Park SA, et al. LFA-1 (CD11a/CD18) and Mac-1 (CD11b/CD18) distinctly regulate neutrophil extravasation through hotspots I and II. Exp Mol Med 2019 Apr 9;51(4):1-13; doi: 10.1038/s12276-019-0227-1.

38. Pulikkot S, Hu L, Chen Y, et al. Integrin Regulators in Neutrophils. Cells 2022 Jun 25;11(13):2025; doi: 10.3390/cells11132025.

39. Saunders NR, Kitchener P, Knott GW, et al. Development of walking, swimming and neuronal connections after complete spinal cord transection in the neonatal opossum, Monodelphis domestica. J Neurosci 1998 Jan 1;18(1):339-55; doi: 10.1523/JNEUROSCI.18-01-00339.1998.

40. Li Y, He X, Kawaguchi R, et al. Microglia-organized scar-free spinal cord repair in neonatal mice. Nature 2020 Nov;587(7835):613-618; doi: 10.1038/s41586-020-2795-6.

41. Anthony DC, Bolton SJ, Fearn S, et al. Age-related effects of interleukin-1 beta on polymorphonuclear neutrophil-dependent increases in blood–brain barrier permeability in rats. Brain 1997 Mar;120 (Pt 3):435-44; doi: 10.1093/brain/120.3.435.

42. Korhonen P, Helenius M, Salminen A. Age-related changes in the regulation of transcription factor NF-kappa B in rat brain. Neurosci Lett 1997 Mar 28;225(1):61-4; doi: 10.1016/s0304-3940(97)00190-0.

43. Mülling K, Fischer AJ, Siakaeva E, et al. Neutrophil dynamics, plasticity and function in acute

neurodegeneration following neonatal hypoxia-ischemia. Brain Behav Immun 2021 Feb;92:234-244; doi: 10.1016/j.bbi.2020.12.012.

44. Saggu R, Schumacher T, Gerich F, et al. Astroglial NF-kB contributes to white matter damage and cognitive impairment in a mouse model of vascular dementia. Acta Neuropathol Commun 2016 Aug 4;4(1):76; doi: 10.1186/s40478-016-0350-3.

45. Zamanian JL, Xu L, Foo LC, et al. Genomic analysis of reactive astrogliosis. J Neurosci 2012 May 2;32(18):6391-410; doi: 10.1523/JNEUROSCI.6221-11.2012.

46. Brambilla R, Bracchi-Ricard V, Hu WH, et al. Inhibition of astroglial nuclear factor kappaB reduces inflammation and improves functional recovery after spinal cord injury. J Exp Med 2005 Jul 4;202(1):145-56; doi: 10.1084/jem.20041918.

Figure Legend

Figure 1. Low expression of inflammatory cytokines and chemokines in the neonatal spinal cord after SCI.

A. mRNA expression levels of *Il-1β*, *Il-6*, and *Tnf-a* at 12 hours after crush injury (n=8). **B.** mRNA expression levels of *Cxcl1*, *Cxcl2*, *Cxcl5*, *Ccl2*, and *Ccl3* (n=8). **P*<0.05, ***P*<0.005.

Figure 2. Neutrophils scarcely infiltrate the neonatal spinal cord after SCI.

A. Flow cytometry analysis of the spinal cord and circulating white blood cells showing the monocyte/macrophage fraction ($CD45^{posi}/CD11b^{posi}/Gr\text{-}1^{nega\text{-}int}$) and neutrophil fraction ($CD45^{posi}/CD11b^{posi}/Gr\text{-}1^{high}$) **B.** Quantification of the number of neutrophils per $1.0*10^7$ events detected by flow cytometry (n=5). **C.** Immunohistochemistry of the spinal cord at 12 hours after crush injury showing $Ly6B.2^+$ neutrophil infiltration in adults, whereas no neutrophil infiltration was observed in neonates. **D.** Quantification of $Ly6B.2^+$ neutrophils by immunohistochemistry (n=5) Scale bars, 500 μm in the left-upper panel, 200 μm in the left-lower panel of **C**, and 20 μm in the magnified view. **P*<0.05.

Figure 3. The expression of astrocytic chemokines via NF-κB activation rarely occurs in neonatal mice after SCI.

A. Representative immunohistochemical staining of $EGFP^+$ astrocytes in the naïve spinal cord of Aldh1l1-EGFP mice. Scale bar, 30 μm. **B.** A representative dot plot graph and the flow cytometry gating strategy on the Aldh1l1-EGFP mouse spinal cord exhibiting a cluster of $EGFP^+$ astrocytes. **C.** mRNA expression levels of *Cxcl1* and *Cxcl2* at 12 hours after crush injury (n=6). **D.** Immunohistochemistry of the spinal cord specimens at 12 hours after crush injury showing intranuclear $p65^+$ ($NF\text{-}κB^+$) astrocytes in the adult crush model. Scale bar, 30 μm. **E.** A Z-stack image

of the adult spinal cord at 12 hours after crush injury showing that p65 is specifically expressed in astrocytes. Scale bar: 20 μm. **F.** Quantification of intranuclear $p65^+$ astrocytes via immunohistochemistry (n=5). **G.** Quantification of the process length of $p65^+$ astrocytes revealed significantly longer processes in adult astrocytes (n=5). *P<0.05, **P<0.005.

Figure 4. Circulating neutrophils in neonatal mice express lower levels of chemokine receptors and adhesion molecules.

A. Histograms obtained from flow cytometry analyses showing the expression of CXCR2 in circulating neutrophils of neonates and adults. **B.** Quantification of the proportion of $CXCR2^+$ neutrophils (n=5). **C.** Histograms obtained from flow cytometry analyses showing the expression of β2 integrin in circulating neutrophils of neonates and adults. **D.** Quantification of the proportion of β2 $integrin^+$ neutrophils (n=5). *P<0.05

Figure 5. Neuronal apoptosis following the inflammatory response after SCI is attenuated in neonatal mice.

A. A representative image of TUNEL staining of the adult spinal cord at 12 hours after crush injury showing $TUNEL^+$ nuclei (red). Scale bar, 10 μm. **B.** TUNEL staining of the spinal cord at 12 hours after crush injury showing the wider distribution of TUNEL-positive cells in the adult spinal cord in comparison to the neonatal spinal cord. Scale bar, 500 μm in adults, 250 μm in neonates. **C.** Quantification of $TUNEL^+$ cells in the spinal cord specimens at 12 hours after crush injury (n=5). **D.** Immunohistochemical staining of the spinal cord specimens at 12 hours after crush injury showing colocalization of intranuclear cleaved caspase-3 with $NeuN^+$ neurons in adults but not in neonates. Scale bar, 20 μm. **E.** Quantification of $NeuN^+$ neurons colocalized with intranuclear cleaved caspase-3 at 12 hours after crush injury (n=5). **F.** Quantification of $NeuN^+$ neurons in the epicenter, 1 mm

rostral, and 1 mm caudal of the lesion at 3 days after crush injury (n=6). *P<0.05, **P<0.005.

Figure 6. Serotonergic axon regeneration accompanied by outstanding functional recovery is observed in neonatal mice.

A. Immunohistochemistry showed the loss of 5-HT^{+} axons in both the neonatal and adult spinal cord at 3 days after crush injury. The regeneration of numerous axons was observed only in neonates at 2 weeks after injury. The asterisks indicate the epicenter of the lesion. Insets show higher magnification of axons caudal to the lesion. Scale bar, 1 mm in adults, 500 μm in neonates. **B.** Quantification of the serotonergic axon density caudal to the lesion (n=5). **C.** Locomotor analysis via the BMS at 7, 14, 28, and 112 days after injury (n =6). **D.** A footprint analysis at 16 weeks after injury showing an adult mouse dragging its hindpaw (green) after forepaw (red) placement. In contrast, the neonate showed coordinated steps. **E.** Quantification of the hind paw rotation angle at 16 weeks after injury (n=5). *P<0.05, **P<0.005.

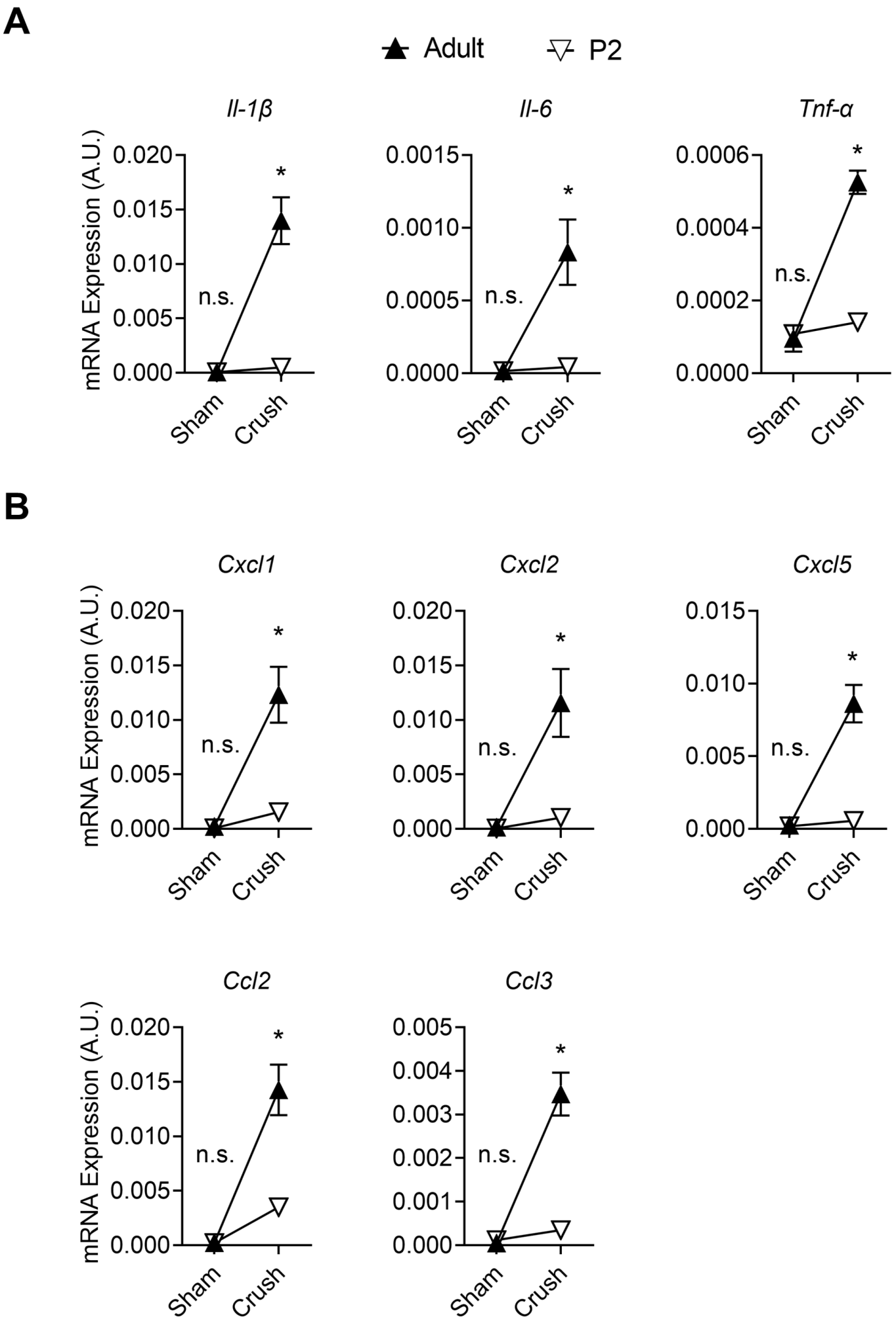
A
Adult
P2
Il-1β
Il-6
Tnf-α
mRNA Expression (A.U.)
0.020
0.015
0.010
0.005
0.000
0.0015
0.0010
0.0005
0.0000
0.0006
0.0004
0.0002
n.s.
*
Sham
Crush
B
Cxcl1
Cxcl2
Cxcl5
Ccl2
Ccl3
0.004
0.003
0.002
0.001

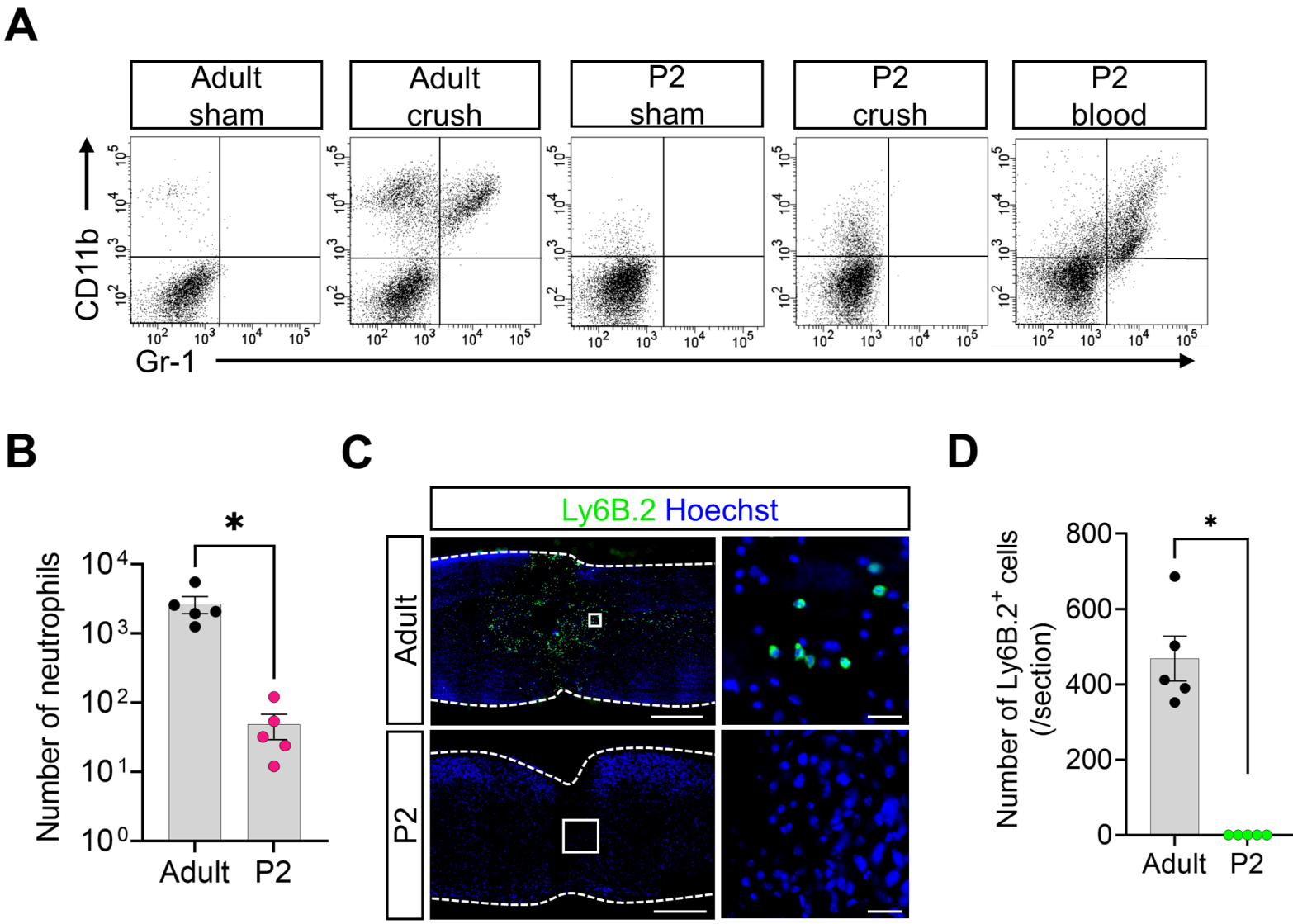
A
Adult sham
Adult crush
P2 sham
P2 crush
P2 blood
CD11b
Gr-1
B
Number of neutrophils
Adult
P2
C
Ly6B.2 Hoechst
Adult
P2
D
Number of Ly6B.2+ cells (/section)
Adult
P2

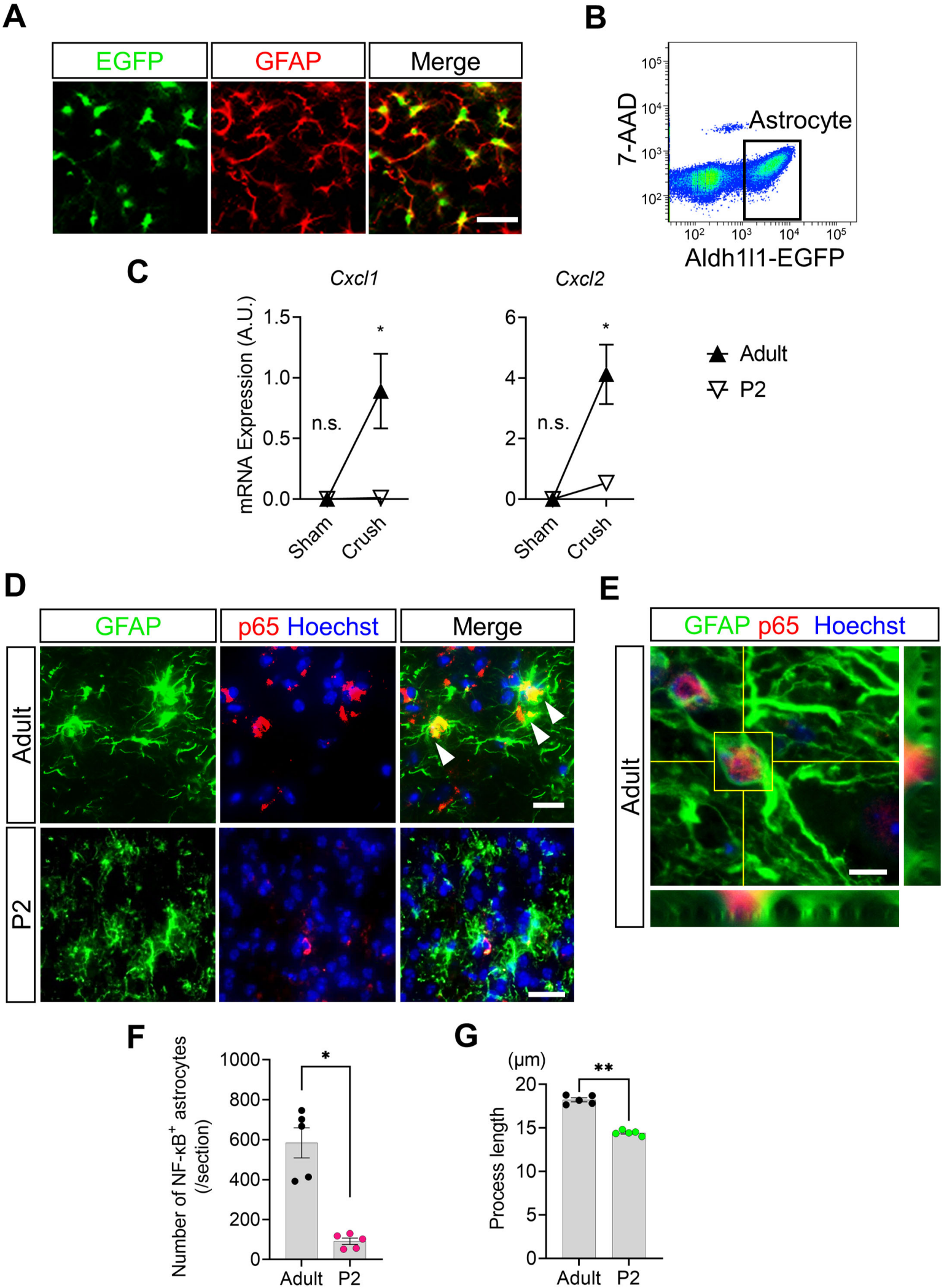
A
EGFP
GFAP
Merge
B
7-AAD
Astrocyte
Aldh1l1-EGFP
C
Cxcl1
Cxcl2
mRNA Expression (A.U.)
n.s.
Sham
Crush
Adult
P2
D
GFAP
p65 Hoechst
Merge
Adult
P2
E
GFAP p65 Hoechst
Adult
F
Number of NF-κB+ astrocytes (/section)
Adult
P2
G
(μm)
Process length
Adult
P2

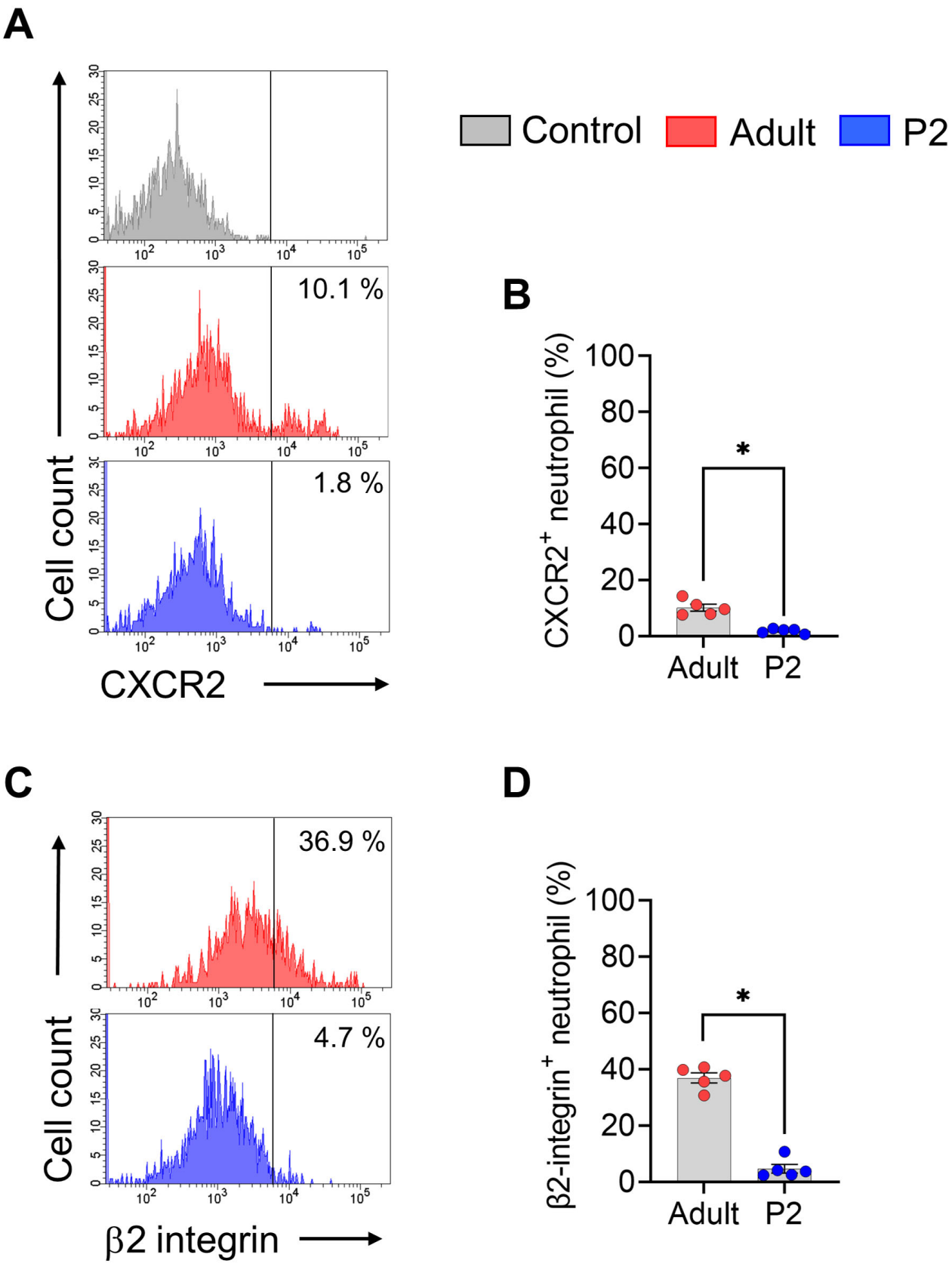
A
Control
Adult
P2
Cell count
10.1 %
1.8 %
CXCR2
B
CXCR2+ neutrophil (%)
100
80
60
40
20
0
*
Adult
P2
C
36.9 %
4.7 %
Cell count
β2 integrin
D
β2-integrin+ neutrophil (%)
100
80
60
40
20
0
*
Adult
P2

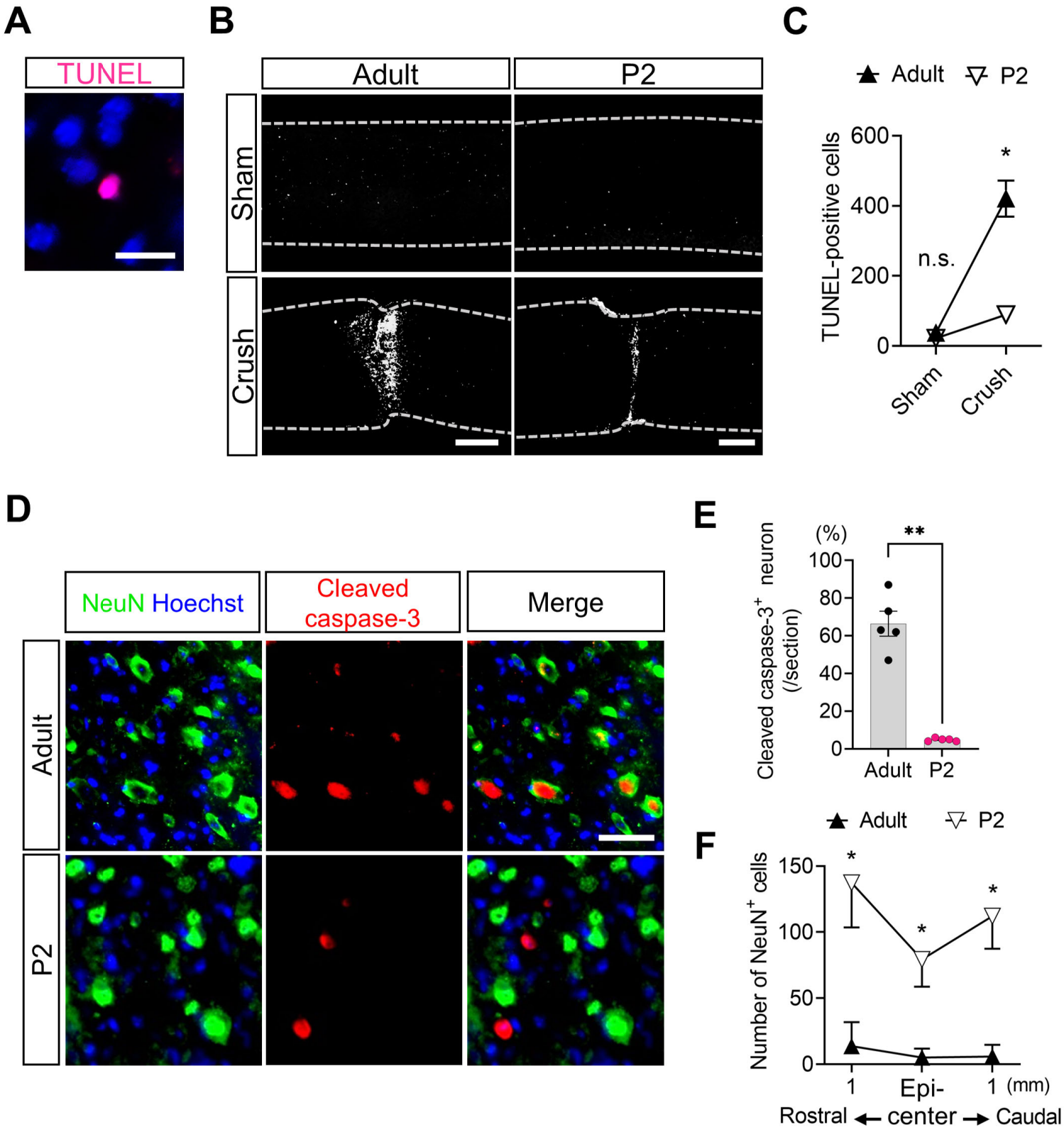
A
TUNEL
B
Adult
P2
Sham
Crush
C
Adult
P2
TUNEL-positive cells
600
400
200
0
n.s.
*
Sham
Crush
D
NeuN Hoechst
Cleaved caspase-3
Merge
Adult
P2
E
(%)
**
Cleaved caspase-3+ neuron (/section)
100
80
60
40
20
0
Adult
P2
F
Adult
P2
Number of NeuN+ cells
150
100
50
0
*
*
*
1
Epi-
1 (mm)
Rostral
center
Caudal

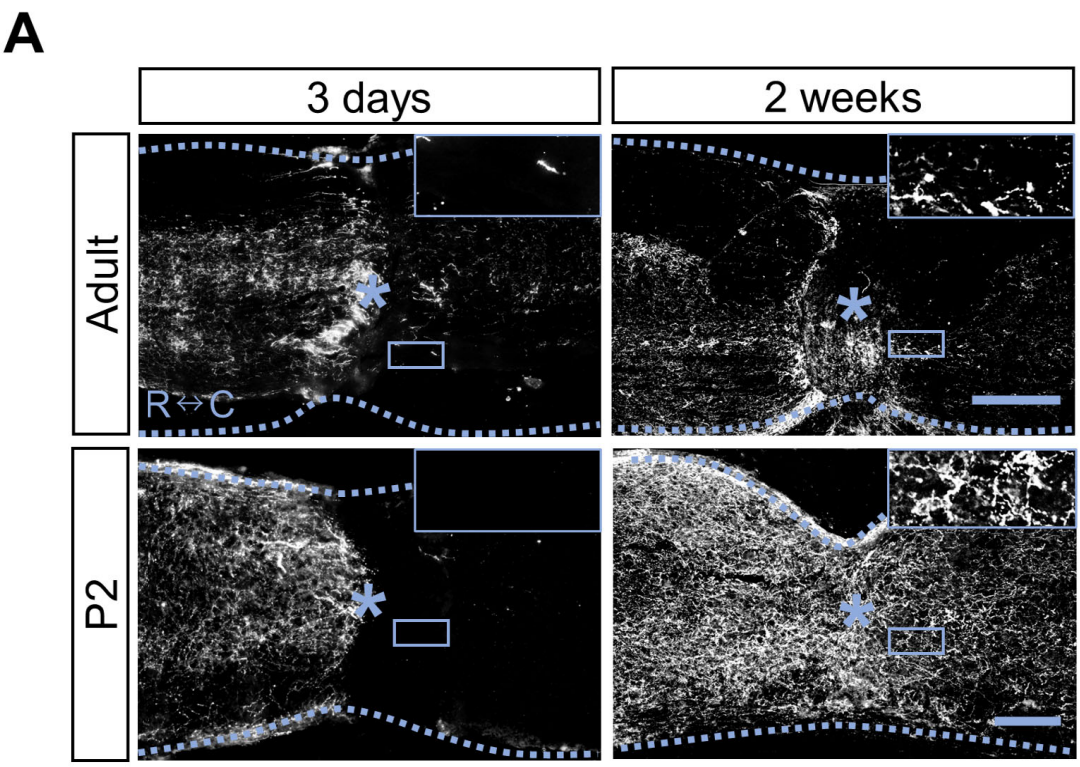
A
3 days
2 weeks
Adult
P2
R↔C

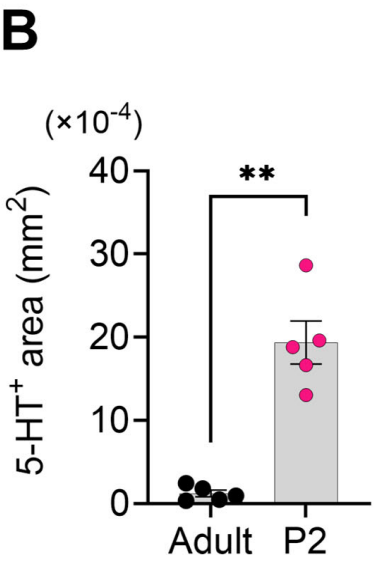
B
(×10-4)
5-HT+ area (mm2)
40
30
20
10
0
**
Adult
P2

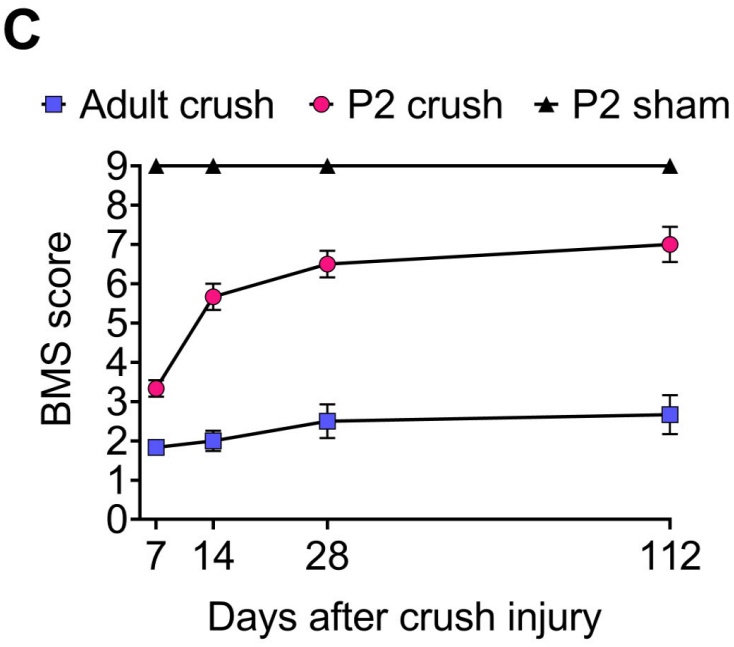
C
Adult crush
P2 crush
P2 sham
BMS score
9
8
7
6
5
4
3
2
1
0
7
14
28
112
Days after crush injury

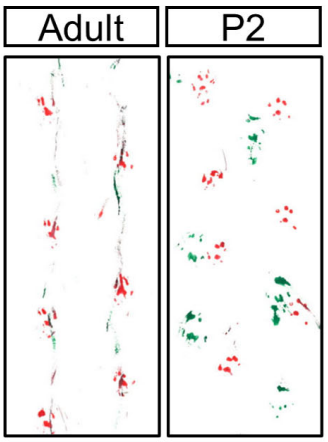
D
Adult
P2

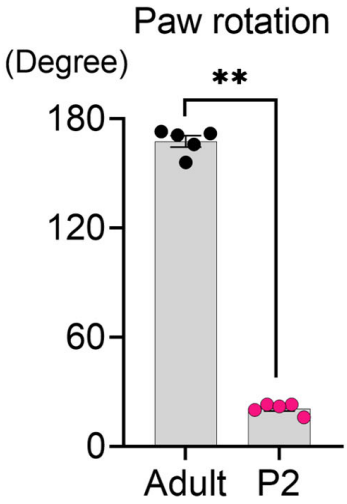
E
Paw rotation
(Degree)
180
120
60
0
**
Adult
P2

Table 1 Primers used in the qPCR analyses

Gene	Accession number	5' – Forward primer – 3'	5' – Reverse primer – 3'
Il-1b	NM_008361.4	CAAAGAGAGCCTGTGTTTTCCTCC	AGCTTCAATGAAAGACCTCAGTGC
Il-6	NM_001314054.1	ACAAGAAAGACAAAGCCAGAGTCC	TATGCTTAGGCATAACGCACTAGG
Tnf-a	NM_001278601.1	TGTGAAAACGGAGCTGAGCTGTCC	GGTTCAGTGATGTAGCGACAGCCT
Cxcl1	NM_008176.3	ACTCAAGAATGGTCGCGAGG	GTGCCATCAGAGCAGTCTGT
Cxcl2	NM_009140.2	AGGGCGGTCAAAAAGTTTGC	CAGGTACGATCCAGGCTTCC
Cxcl5	NM_009141.3	GCACTCGCAGTGGAAAGAAC	CGTGGGTGGAGAGAATCAGC
Ccl2	NM_011333.3	GACCCCAAGAAGGAATGGGT	ACCTTAGGGCAGATGCAGTT
Ccl3	NM_011337.2	GCTGTTTGCTGCCAAGTAGCCACA	CCAAACAGTGTGACCAACTGGGAG
Gapdh	NM_001289726.2	ATGAATACGGCTACAGCAACAGGG	GTCTGGGATGGAAATTGTGAGGGA

Table 2 Results of post-hoc power analyses

			Alpha 0.05, two-sided	
Groups	Number of animals per group	Mean of adult group (± SD)	Mean of P2 group (± SD)	Power (%)
Fig 1A (*Il-1b*: adult crush vs P2 crush)	8	0.013966875 ± 0.006107508	0.000494875 ± 0.000303239	100
Fig 1A (*Il-6*: adult crush vs P2 crush)	8	0.000832365 ± 0.000637345	0.0000417075 ± 0.0000396874	93.8
Fig 1A (*Tnf-α*: adult crush vs P2 crush)	8	0.000525 ± 0.0000907855	0.0001401 ± 0.0000569799	100
Fig 1B (*Cxcl1*: adult crush vs P2 crush)	8	0.012316551 ± 0.007264585	0.001541131 ± 0.001370872	98.5
Fig 1B (*Cxcl2*: adult crush vs P2 crush)	8	0.01155394 ± 0.008821107	0.00102708 ± 0.000680927	92.0
Fig 1B (*Cxcl5*: adult crush vs P2 crush)	8	0.00861828 ± 0.003655494	0.000556729 ± 0.000397166	100
Fig 1B (*Ccl2*: adult crush vs P2 crush)	8	0.014252256 ± 0.006579871	0.003484126 ± 0.001840541	99.4
Fig 1B (*Ccl3*: adult crush vs P2 crush)	8	0.003467938 ± 0.001392704	0.000348744 ± 0.00015441	100
Fig 2B (Number of neutrophils: adult vs P2)	5	2672.6 ± 1663.01	48.6 ± 43.2759	94.1
Fig 2D (Number of Ly6B.2$^+$ cells: adult vs P2)	5	468.6 ± 133.6255964	0	100
Fig 3C (Astrocyte *Cxcl1*: adult crush vs P2 crush)	6	0.890993901 ± 0.754186626	0.010427034 ± 0.16076436	79.9
Fig 3C (Astrocyte *Cxcl2*: adult crush vs P2 crush)	6	4.124127667 ± 2.407287698	0.5356095 ± 0.225868648	95.3
Fig 3F (Number of NFκB$^+$ astrocytes: adult vs P2)	5	584 ± 168.1978002	92 ± 35.5879193	100
Fig 3G (Process length: adult vs P2)	5	18.225 ± 0.505284573	14.42 ± 0.290150823	100
Fig 4B (CXCR2$^+$ Neutrophils: adult vs P2)	5	10.12 ± 2.747180373	1.82 ± 0.85264295	100
Fig 4B (β2-integrin$^+$ Neutrophils: adult vs P2)	5	36.9 ± 3.988107321	4.68 ± 3.445576875	100
Fig 5C (TUNEL$^+$ cells: adult crush vs P2 crush)	5	420.8 ± 115.4673114	89.4 ± 17.9248431	100
Fig 5E (Cleaved caspase-3$^+$ neurons: adult vs P2)	5	66.4 ± 14.79188967	4.8 ± 0.836660027	100
Fig 5F (Number of NeuN$^+$ cells at epicenter: adult vs P2)	6	5 ± 6.870225615	79.33333333 ± 20.67526703	100
Fig 5F (Number of NeuN$^+$ cells at 1 mm rostral: adult vs P2)	6	13.66666667 ± 18.08498456	137.3333333 ± 33.77967831	100
Fig 5F (Number of NeuN$^+$ cells at 1 mm caudal:	6	5.833333333 ± 8.886319073	112 ± 24.60081299	100

adult vs P2)				
Fig 6B ($5HT^+$ area: adult vs P2)	5	1.2156 ± 0.906946691	19.358 ± 5.783763481	100
Fig 6C (BMS score at day 7: adult crush vs P2 crush)	6	1.833333333 ± 0.40824829	3.333333333 ± 0.516397779	100
Fig 6C (BMS score at day 14: adult crush vs P2 crush)	6	2 ± 0.632455532	5.666666667 ± 0.816496581	100
Fig 6C (BMS score at day 28: adult crush vs P2 crush)	6	2.5 ± 1.048808848	6.5 ± 0.836660027	100
Fig 6C (BMS score at day 112: adult crush vs P2 crush)	6	2.666666667 ± 1.211060142	7 ± 1.095445115	100
Fig 6E (Paw rotation: adult vs P2)	5	167.6 ± 7.0214	20.8 ± 2.94958	100

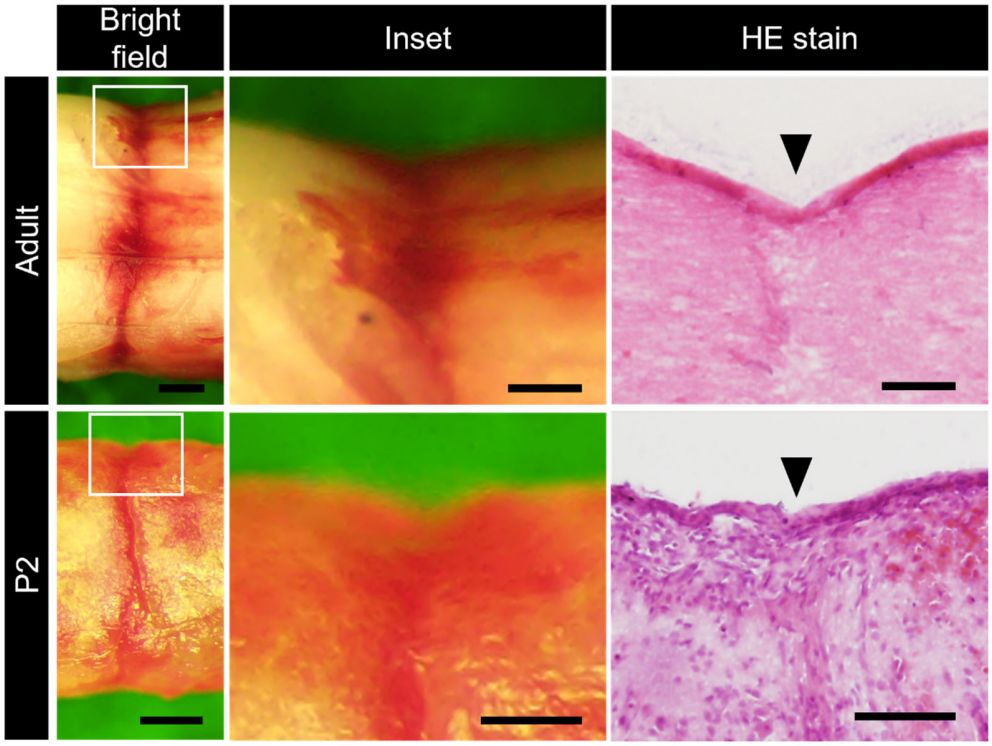

The spinal cord of adult and neonates immediate after crush injury. Images were captured from the ventral side of the spinal cord. Both the bright field capture and HE-stained images show that the dura mater was not affected by the crush injury. Arrowheads indicate the lesion epicenter. Scale bar: 500 μm (left panels), 200 μm (center panels and right panels).

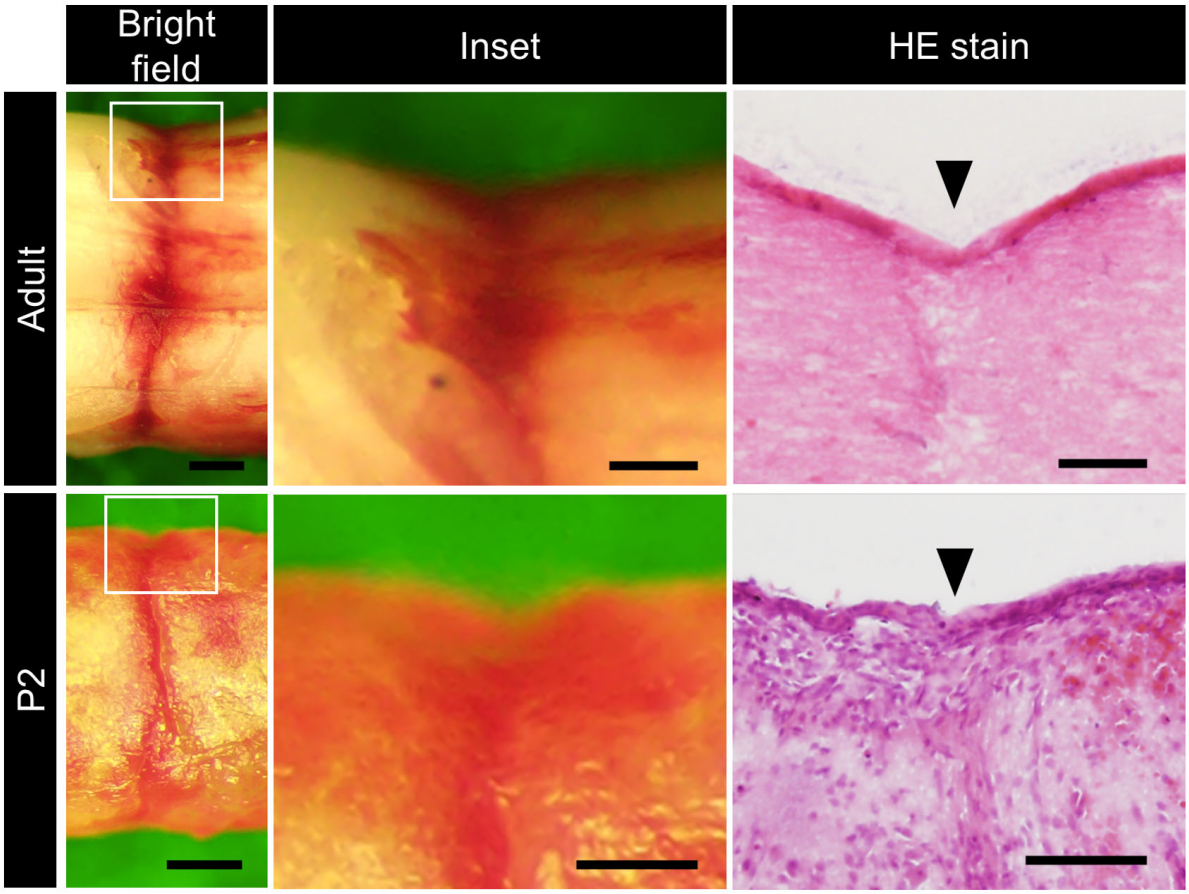
Bright field
Inset
HE stain
Adult
P2